A Micromachined Ultrasonic Power Receiver for Biomedical Implants

Hamid Basaeri*[a], and Shad Roundy[a]
[a]University of Utah, Dept. of Mech. Eng., 1495 E 100 S, Salt Lake City, UT 84112, USA;

ABSTRACT

Bio-implantable medical devices need a reliable and stable source of power to perform effectively. Although batteries can be the first candidate to power implantable devices as they provide high energy density, they cannot supply power for long periods of time and therefore, they must be periodically replaced or recharged. Battery replacement is particularly difficult as it requires surgery. In this paper, we develop a micromachined ultrasonic power generating receiver with a size of $3.5mm \times 3.5mm$ capable of providing sufficient power for implantable medical devices. The ultrasound receiver takes the form of a unimorph diaphragm consisting of PZT on silicon. We dice bulk PZT with a thickness of 127 μm and bond the diced pieces to a silicon wafer. In order to get a 50 μm thick PZT layer, which is needed for optimal power transfer, we mechanically lap and polish the bonded PZT. We numerically investigate the performance of the fabricated receiver with inner and outer electrodes on the surface of the PZT. Using COMSOL simulations, we analyze the effect of different sizes of inner and outer electrodes under the actuation of the inner electrode in order to find the optimum electrode sizes. We show that when the transmitter is generating an input power less than Food and Drug Administration limits, the receiver can provide sufficient voltage and power for many implantable devices. Furthermore, the process developed can be used to fabricate significantly smaller devices than the one characterized, which enables further miniaturization of bio-implanted systems.

Keywords: Acoustic power transfer; MEMS; medical implantable devices

1. INTRODUCTION

The lack of very small, long-term power sources has become a practical issue for implantable medical devices (IMDs). If batteries are used, surgery may be required to replace the batteries every few years. Researchers have found several ways to mitigate this problem by using wireless power transfer technologies as an alternative to batteries. Mid to far field radio frequency (RF) radiation and inductive power transfer (IPT) are the first approaches to wirelessly power IMDs due to their ease of application [1]. However, short transfer distances and low efficiencies resulting from high attenuation in the human body limit their range of application.

Acoustic power transfer has several advantages over other methods and can be a safe way to power implantable devices. Denisov and Yeatman have shown that this method can be more efficient than inductive power transfer for small sizes and large implant depths [2]. Moreover, acoustic energy has much shorter wavelengths and its attenuation is relatively low in human tissue compared to RF. For a more detailed discussion of acoustic power transfer for IMDs, we refer the reader to [3].

Plate and diaphragm architectures are two common ultrasonic power receiver structures. Although the plate is the more widely used architecture in generating and receiving acoustic waves, the diaphragm can be a better candidate for powering a bio-implantable device because it can be smaller for a given operating frequency. In this paper, we design and fabricate a micromachined ultrasonic power receiver based on a diaphragm structure. After briefly comparing two common structures, we discuss the fabrication process and present the preliminary results of the device characterization.

2. DESIGN CONCEPT

Piezoelectric transduction is one of the most common ways to convert acoustical energy into electrical energy and vice-versa. There are two piezoelectric generator architectures that may be used for acoustic power transfer as shown in Figure 1: the bulk-mode plate and the flexure-mode unimorph diaphragm. The plate which operates in thickness mode is a circular piezoelectric disk that is rigidly fixed around its circumference. The polling axis of this architecture, the piezoelectric 3–3 axis, is perpendicular to the face of the plate. The diaphragm architecture is a circular piezoelectric disk fixed to the back

* h.basaeri@utah.edu

Active and Passive Smart Structures and Integrated Systems 2017, edited by Gyuhae Park, Alper Erturk, Jae-Hung Han, Proc. of SPIE Vol. 10164, 1016416
 · doi: 10.1117/12.2260059

side of a larger circular non-piezoelectric shim. The shim is usually fixed around its circumference. In this structure, the strain in the piezoelectric disc is dominant in the 3-1 direction (bending). A single piezoelectric layer (i.e. a unimorph), or a piezoelectric layer on each side of the shim (i.e. a bimorph) can both be employed for diaphragm architectures. The piezoelectric layer can either partially cover the shim or cover the entire surface of the shim and employ patterned electrodes on the piezo surface.

Figure 1. Plate (left) and diaphragm (right) architectures [3].

For the thickness mode, the first resonance frequency of the plate is a function of its thickness h, and its frequency constant N_{th}, and can be written by:

$$f_r^t = \frac{N_{th}}{h} \tag{1}$$

Based on Eq. (1), increasing the operating frequency would result in a thinner plate to operate at resonance. The plate is used as a transmitter in a broad range of applications such as diagnostic and therapeutic ultrasound. At the centimeter to millimeter scale, this structure has high acoustic power output that makes it an appropriate choice for high acoustic to electrical power generation. As mentioned above, the diaphragm operates in the 3-1 mode which has a lower coupling coefficient than the 3-3 mode of the plate. However, the diaphragm can operate at much lower frequencies than the plate, and this make it a better candidate in bio-implantable power applications.

Frequency plays an important role in determining the size of the receiver. Considering the fact that the thickness of the receiver is smaller than its diameter, using diaphragm structures would result in smaller devices compared to plate structures when operating at the same frequency. In other words, diaphragm architectures are capable of operating at lower frequencies compared to plate architectures for the same size. Furthermore, frequency can also affect some other parameters in the system. The higher the frequency, the higher the attenuation.

Another important issue for implantable power receivers is their sensitivity to offset and alignment mismatches between the transmitter and receiver. In some cases, a lateral offset equal to the diameter of the receiver may result to approximately %70 drop in the generated voltage [4]. The drop could also be worse for the generated power as it is a function of voltage squared. Operating at lower frequencies which have longer wavelength can result in devices that are less sensitive to offset and alignment mismatches. Christensen and Roundy [5] compared plate and diaphragm mode structures for an acoustic power transmission system and showed that the diaphragm structure is significantly less sensitive to changes in implant offset and angle.

In this work, we choose a diaphragm structure as a receiver for powering implantable devices. To improve the generated voltage of the receiver, we used patterned electrodes on top of the PZT. Our presented device has piezoelectric material over the entire structure, however, unlike off-the-shelf diaphragms, it has separate inner and outer electrodes instead of a single center electrode. Figure 2 illustrates a 3D schematic of the cross section of the ultrasonic receiver with patterned inner and outer electrodes. The idea behind using inner and outer electrodes is that when the acoustic pressure is applied to the receiver, the inner (outer) portion of the diaphragm will be in tension while the outer (inner) portion will be in compression [6].

Although piezoelectric materials are widely employed in a variety of macroscale devices, their integration into microelectromechanical (MEMS) devices has been challenging. Among different piezoelectric materials, PZT exhibits high piezoelectric coefficients, d_{33}, d_{31}, and coupling coefficients. There are several deposition techniques for integration of piezoelectric materials on silicon, however, there are extreme challenges in getting a PZT layer with a thickness more

than 5 μm. Moreover, the devices that result from deposited PZT typically suffer from low piezoelectric coefficients compared to bulk piezoelectric materials. As bulk piezoelectric materials provide much more electromechanical force due to the simple fact that they contain more piezoelectric material, maximum power generation is usually obtained with bulk materials rather than thin-film deposited piezoelectric materials. Therefore, in this work, we start with bulk PZT with a thickness of 127 μm and polish it back to get a PZT layer that is thicker than standard microfabrication processes, but thin enough for a millimeter scale bending diaphragm (i.e. 20 – 50 μm).

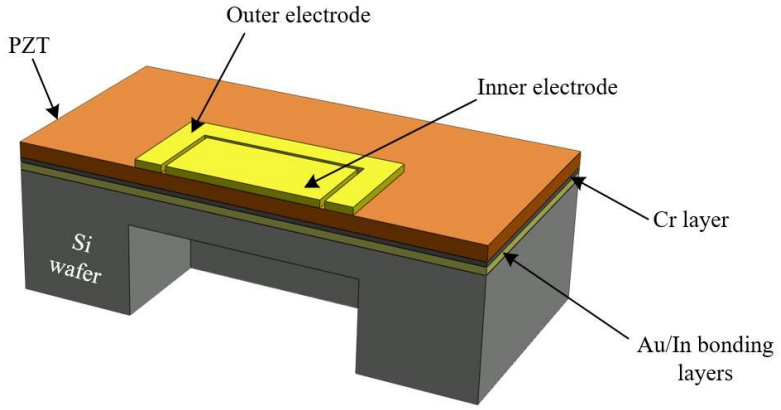

Figure 2. schematic drawing showing the cross-sectional view of the proposed micromachined ultrasonic receiver.

3. MODELING AND SIMULATION

The results of this paper are based on simulation models that include experimental data to evaluate the accuracy of results. COMSOL Multiphysics software is used for all simulations in this paper.

3.1 Modeling Validation

To validate COMSOL simulations, an off-the-shelf diaphragm transducer (Steminc, SMPD11D11T10F95) was mounted to a cylindrical housing as shown in Figure 3. This structure was then modeled as a standalone transmitter. A sinusoidal input from a function generator at 2.5 V amplitude was applied to the electrodes of the transducer and the diaphragm's displacement was measured by a laser vibrometer. The frequency was swept between 1 Hz and 10 kHz. The results from simulation closely match the experimental data as shown in Figure 4.

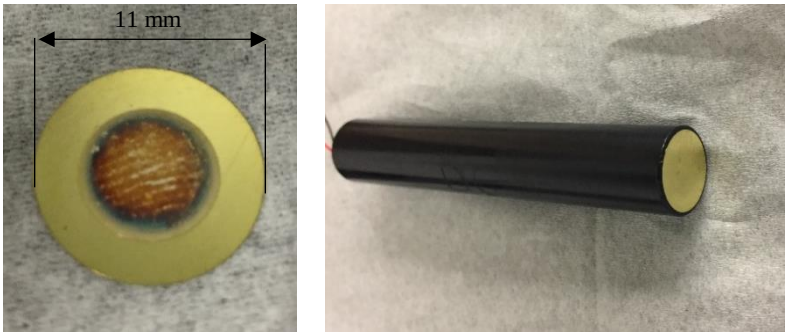

Figure 3. left) off-the-shelf diaphragm transducer, right) diaphragm transducer mounted to a cylindrical housing.

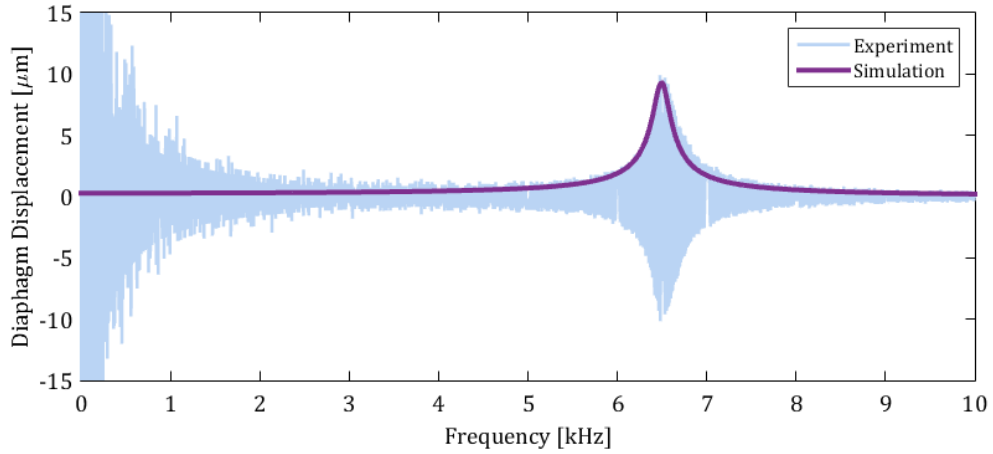

Figure 4. Simulation and experimental results for a diaphragm transducer tested as stand-alone transmitter.

As a second validation of the COMSOL model, two diaphragm transducers were placed in water separated by 1 cm. The first, the transmitter, was excited by a 2.5 V amplitude voltage which was swept from 1 Hz to 10 kHz. The resulting acoustic wave excited the second diaphragm (i.e the receiver). The voltage generated on the receiver was monitored across a 100 Ω load. Figure 5 shows simulation and experimental results of the full power transmission model. As shown in the figure, there is good agreement between model and experiment. It is clear that the simulation data has only one peak while there are two peaks in the experimental results. This is due to the fact that, in the experiments, the two transducers are not exactly the same and have slightly different resonance frequencies because of manufacturing variation, or mounting differences.

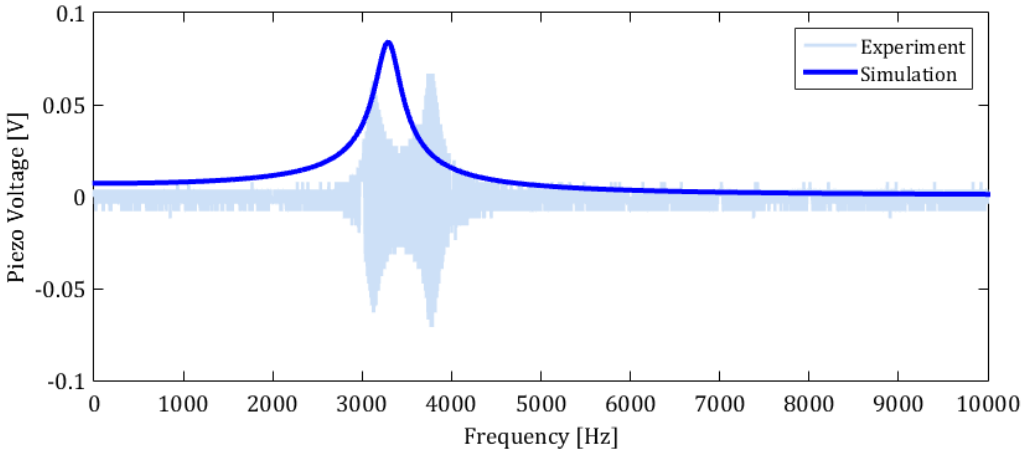

Figure 5. Simulation and experimental results for diaphragm to diaphragm acoustic power transmission.

3.2 Simulation comparison

A silicon diaphragm structure with a piezoelectric layer that does not cover the entire surface of the diaphragm (see Figure 1) was first simulated. In this case, the piezoelectric material has a smaller diameter than the diaphragm. For a diaphragm structure with a diameter of 2 *mm*, silicon thickness of 50 μm, and piezoelectric material thickness of 20 μm, the piezoelectric diameter was varied from 200 μm to 2 *mm*. The top and bottom surfaces of the piezoelectric material act as the two electrodes and there are no patterned electrodes in this structure. A static pressure of 98 *kPa* was applied to the diaphragm. This pressure is calculated based on the limitations on the input power intensity to human body set by Food and Drug Administration (FDA) [7]. We used this limit (720 mW/cm^2) as the power intensity of the transducer outside the

body. Knowing the acoustic impedance of the tissue and the power intensity, we calculated the pressure at the transmitter face. The static pressure of 98 *kPa* is the pressure at the receiver face when the attenuation is considered for the input pressure. The generated power as a function of the ratio of piezoelectric material diameter to diaphragm diameter is shown in Figure 6.a. As the piezoelectric diameter increases, the power initially increases. At some diameter, the power begins to decrease as the strain in the outer portion of the piezo material is of opposite sign to the strain on the inner portion and counteracts the voltage generation. Although these simulations were carried out for circular diaphragms, we still can take advantage of the results of the electrode ratio for other kinds of diaphragms. For a square diaphragm, we used the electrode ratio results from the circular diaphragm and applied the results to the electrodes' length ratio.

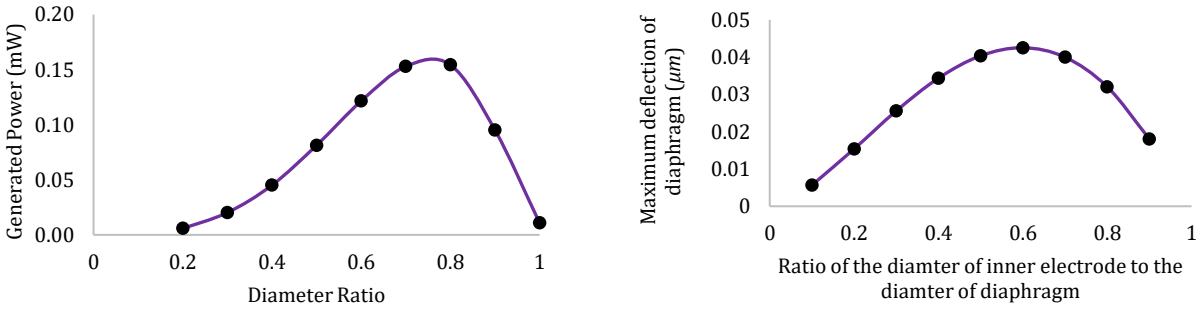

a) b)

Figure 6. a) Effect of piezoelectric material diameter on the generated power, b) Effect of the diameter of the inner electrode on the maximum deflection of the diaphragm.

A second simulation was performed for the case where the entire diaphragm structure is covered with piezoelectric material and the top surface is partitioned into an inner and outer electrode (see Figure 7 as an example of this structure for a square diaphragm). The piezoelectric material covers the entire diaphragm. The bottom surface of the piezoelectric material does have a conductive electrode, but it is not accessible. The effect of the ratio of the inner electrode to outer electrode diameters was investigated via simulation. A voltage of 3 *V* was applied to the inner electrode and the outer electrode acted as ground. The simulation results are presented in Figure 6.b for different inner electrode sizes in order to get an idea of its optimized size. The gap between two top electrodes is set to be 10 μm. These simulations show that for a fixed value of source voltage, there would be an electrode size ratio which results in maximum deflection of the diaphragm. Although the diaphragm structure is operating in reverse-mode by driving it with an applied voltage and measuring the deflection, it is believed that these results should be indicative of the ability of the diaphragm to generate voltage under a deflection. Therefore, the optimum size of electrodes would result in getting higher power.

4. FABRICATION

The design of a square shaped d_{31}-mode ultrasonic piezoelectric receiver is shown in Figure 7. The device was fabricated at the wafer- level by slightly modifying a previously published process [8]. Dimensions of inner and outer electrodes are selected based on the FEA simulations. The three-mask fabrication process includes deposition of bonding layer metals, bonding, mechanical lapping, deposition of electrodes (Cr/Au), and release of diaphragm structures by back-side etching of the Si wafer. The fabrication process starts with deposition of the bonding layer metals (Au/In) on the bulk PZT and Silicon wafer. Then, the PZT sheet is diced into small square pieces of the desired size. The PZT pieces were then bonded to the silicon wafer using a heated platen press with a bonding pressure of 0.75 *MPa* at 188˚C for 1 hour. One challenge of bonding the bulk PZT layers is that the commercial PZT layers have rough surface which may result to poor bonding. The other important issue is the bonding temperature should be well below the Curie temperature (350˚C). High bonding temperatures would lead to loss of polarization in the piezoelectric material. Mechanical lapping and polishing processes were performed to decrease the thickness of the bulk PZT from 127 μm to ~25 μm. The diaphragm was created by back-side Deep Reactive Ion Etch (DRIE). Finally, the top electrodes are patterned by sputtering and lifting off of Cr/Au. Figure 8 shows the fabricated device.

Figure 7. Schematic of micromachined ultrasonic receiver, left) top view, right) side view.

Figure 8. Fabricated micromachined ultrasonic receiver.

5. EXPECTED RESULTS

The expected voltage and power from the piezoelectric micromachined receiver are shown Figure 9. This figure illustrates that the resonance frequency of the device would be 75 *kHz*, and the peak received voltage would be 2.11 volts (0-pk). It is assumed that the transmitter generates a power density equal to 720 mW/cm^2 and the distance between the receiver and the transmitter is 1 *cm*. Using an optimal resistive load, the device would be capable of producing 3.42 *mW* of power. We designed the diaphragm for a silicon thickness of 50 μm. However, due to over-etching of the backside silicon, the silicon layer underneath the PZT was much thinner than 50 μm. Therefore, we could not experimentally validate these simulation results. The backside silicon was almost completely etched away during the backside etching process. The silicon thickness is a key factor in determining the resonance frequency as well as voltage and power generation. We further expect that this diaphragm based receiver will be far less sensitive to alignment and orientation mismatches compared to a bulk mode receiver due to the lower resonance frequency, and thus longer wavelengths relative to device size.

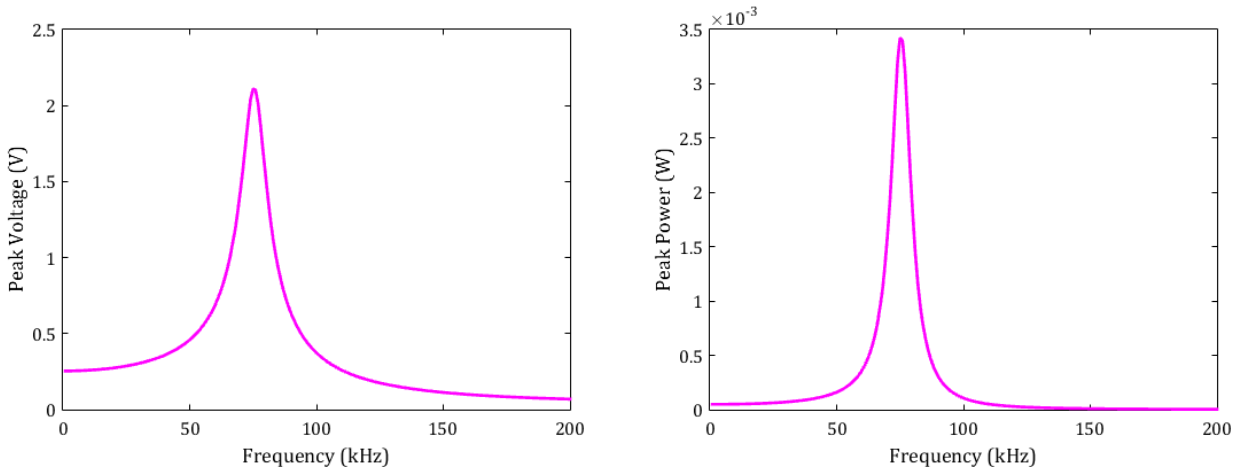

Figure 9. Expected performance of the receiver, left) voltage, right) power.

6. CONCLUSION

In this paper, we presented the design, simulation, and fabrication process of a piezoelectric (PZT) micromachined ultrasonic power receiver for implantable devices. Simulations were carried out to analyze the effect of separate inner and outer electrodes instead of a center electrode covering the entire surface of PZT. We found the optimum sizes for electrodes at which the deflection of the diaphragm would be maximum and used this value to fabricate our device. We used bulk PZT because it is able to provide much more electromechanical force compared to deposited piezoelectric material. Using mechanical lapping and polishing processes, we decreased the thickness of the PZT from 127 μm to ~25 μm.

Future work includes improving the manufacturing process for more reliable thickness control of the diaphragm. This includes front side polishing and backside etching. Newly fabricated devices will be experimentally characterized in water for power vs. depth, alignment and orientation and compared to predictive models.

7. ACKNOWLEDGEMENT

This work was supported by National Science Foundation under Award Number ECCS 1408265.

REFERENCES

[1] Amar, A. Ben., Kouki, A. B.., Cao, H., "Power approaches for implantable medical devices," Sensors (Switzerland) **15**(11), 28889–28914 (2015).

[2] Denisov, A.., Yeatman, E., "Ultrasonic vs. Inductive Power Delivery for Miniature Biomedical Implants," 2010 Int. Conf. Body Sens. Networks, 84–89 (2010).

[3] Basaeri, H., Christensen, D. B.., Roundy, S., "A Review of Acoustic Power Transfer for Bio-Medical Implants," Smart Mater. Struct. **25**(12), 123001, IOP Publishing (2016).

[4] Basaeri, H., Christensen, D., Yu, Y., Nguyen, T., Tathireddy, P.., Young, D. J., "Ultrasonically Powered Hydrogel-Based Wireless Implantable Glucose Sensor," 2016 IEEE Sensors Proc., 1–3 (2016).

[5] Christensen, D. B.., Roundy, S., "Ultrasonically powered piezoelectric generators for bio-implantable sensors: Plate versus diaphragm," J. Intell. Mater. Syst. Struct. **27**(8), 1092–1105 (2016).

[6] Kim, S., Clark, W. W.., Wang, Q., "Piezoelectric energy harvesting using a diaphragm structure," Smart Struct. Mater. **5055**, 307–318 (2003).

[7] "Guidance for Industry and FDA Staff Information for Manufacturers Seeking Marketing Clearance of Diagnostic Ultrasound Systems and Transducers.", Silver Spring US FDA (2008).

[8] Aktakka, E. E., Peterson, R. L.., Najafi, K., "Wafer-level integration of high-quality bulk piezoelectric ceramics on silicon," IEEE Trans. Electron Devices **60**(6), 2022–2030 (2013).